Modelling of Mercury's surface composition and remote detection from the orbit with the BepiColombo Mercury Planetary Orbiter

H. Lammer[1], P. Wurz[2], J.A.M. Fernández[3], H.I.M. Lichtenegger[1], and M. L. Khodachenko[1]
[1]Austrian Academy of Sciences, Space Research Institute, Schmiedlstr. 6, A-8042 Graz, Austria
helmut.lammer@*oeaw.ac.at, Herbert.lichtenegger@oeaw.ac.at, maxim.khodachenko@oeaw.ac.at*
[2]Physikalisches Institut, Universität Bern, Sidlerstrasse 5, CH-3012 Bern, Switzerland
peter.wurz@soho.unibe.ch
[3]Department for Computer Science and Applied Mathematics, University of Girona, Edifici, P-IV,
Campus Montilivi, E-17071 Girona
josepantoni.martin@udg.edu

Abstract

It can be assumed that the composition of Mercury's thin gas envelope (exosphere) is related to the composition of the planets crustal materials. If this relationship is true, then inferences regarding the bulk chemistry of the planet might be made from a thorough exospheric study. The most vexing of all unsolved problems is the uncertainty in the source of each component. Historically, it has been believed that H and He come primarily from the solar wind, while Na and K originate from volatilized materials partitioned between Mercury's crust and meteoritic impactors. The processes that eject atoms and molecules into the exosphere of Mercury are generally considered to be thermal vaporization, photon-stimulated desorption (PSD), impact vaporization, and ion sputtering. Each of these processes has its own temporal and spatial dependence. The exosphere is strongly influenced by Mercury's highly elliptical orbit and rapid orbital speed. As a consequence the surface undergoes large fluctuations in temperature and experiences differences of insolation with longitude. We will discuss these processes but focus more on the expected surface composition and solar wind particle sputtering which releases material like Ca and other elements from the surface minerals and discuss the relevance of composition modelling.

Kew words: Mercury, surface mineralogy, composition modelling, exosphere

1 Introduction

Mercury is the less investigated and studied planet in the Solar System, because the only information which was obtained from spacecraft comes from three fly-bys performed in 1974 by the Mariner 10 spacecraft and a recent flyby (14 January 2008) by NASA`s Messenger spacecraft. Ground-based observations provided interesting results, they are difficult to obtain due to the planet' closeness to the Sun. One Mercury day correspond to 58.785 Earth's days, which is 2⁄3 of the planets orbital period. The surface temperature at the dayside ranges from 700 K at the subsolar point up to 90 K in the aphelion midnight point. The planetary radius is about 2440 km which is about 2.6 times smaller than that of the Earth. The uncompressed density is the highest for solar system planets and is about 5.3 g cm^{-3} (Lewis, 1988). The reason is that Mercury has a large iron core. It is likely that the innermost planet in the solar system has had a peculiar evolutionary history. The Mariner 10 fly-bys discovered the existence of an intrinsic magnetic field (Ness et al., 1974; 1976). Although the magnetic field estimation has large uncertainties Mercury's magnetic dipole moment could be estimated between 200 - 400 nT R^3_M with the dipole axis approximately aligned with its spin axis. Compared to Mercury's magnetic moment the Earth's magnetic moment of about 30,000 nT R^3_E is much higher.

Mariner 10 reported also no observational evidence of a proper atmosphere, however, a thin gaseous envelope around the planet was observed (Broadfoot et al., 1976). This thin gaseous envelope is an exosphere where the neutral atoms/molecules move in a collision-less medium (e.g., Wurz and Lammer, 2003; Killen et al., 2007). Moreover, the planet's surface interacts in a complex manner with the particle flux and radiation environment of the Sun. These scenarios are illustrated in Figure 1. A detailed study of the various exospheric species can provide important information about the planet`s surface composition and its evolution. Mercury`s exosphere is continuously eroded and refilled by these Sun-driven plasma and radiation interaction processes, so that one can consider the environment as a single, connected "surface-exosphere-magnetosphere" system. These three regions are strongly linked to each other. Besides NASA`s Messenger mission the European Space Agency`s (ESA) cornerstone mission together with Japan (JAXA), BepiColombo, to be launched in 2013, have stimulated new interest in the planetary community.

From observations with the UVS-instrument on Mariner 10 only H, He and O were observed in Mercury's exosphere (Broadfoot et al., 1976). Potter and Morgan (1985) performed ground-based observations and discovered strong emission features at the Fraunhofer Na D lines in Mercury's spectrum attributed to resonant scattering of sunlight from Na vapour in the planetary exosphere. They estimated a Na column density of 8.1×10^{15} m^{-2}, which later was reduced to $1 - 3 \times 10^{15}$ m^{-2} (Killen and Morgan, 1993). Later suprathermal Na in Mercury's exosphere has been observed by Potter and Morgan (1997a). A detailed investigation of Na line profiles by Killen et al. (1999) revealed that gas is hotter than the planets surface by 600 – 700 K. Potter and Morgan discovered also small concentrations of K in Mercury's exosphere, about a factor of 200 less than Na (Potter and Morgan, 1997b). Ca was discovered as the 6th element in Mercury's exosphere, and its existence in the exosphere was attributed to sputtering because of its proximity to Mercury's poles, where solar wind protons can enter the magnetic field configuration (Bida et al., 2000). Diurnal variations of Na and K column abundances have been observed (Sprague et al., 1997), with morning and midday Na column abundances a factor of 3 larger than in the afternoon. An additional unexpected discovery was made by radar observations of Mercury where bright regions near the polar areas were discovered (Harmon and Slade, 1992). These areas could be indications for the presence of condensed volatile species analogous to that suggested for permanently shadowed regions on the Moon. They were originally attributed to H_2O ice (Harmon and Slade, 1992). Contrary to that it has been suggested that cold silicate minerals would also produce similar results (Starukhina et al., 2000). The chemical nature of such volatile deposits on Mercury was proposed to be either water-ice (Harmon and Slade, 1992; Harmon et al., 2001), elemental S (Sprague et al., 1995), or Na (Harmon and Slade, 1992). Remote observations of Mercury's surface using X-ray and optical spectroscopy as well as in situ measurements of the exosphere composition from ESA's Mercury Planetary Orbiter (MPO) of the BepiColombo mission should resolve the controversy and help to explain the cycling of volatile elements between Mercury's interior, surface mineralogy and exosphere, and the contribution of meteoritic and cometary material to Mercury's near-surface volatile budget.

A main reason for the interest in Mercury's exosphere, its composition and the processes responsible for populating and removing material from it is because exospheric material directly originates from the planetary surface. In the absence of a Lander which investigates Mercury's surface composition in situ, the exosphere composition can be measured with mass spectrometers at the orbit.

There are four physical processes responsible for releasing surface material into the exosphere (e.g. Lammer at al., 2003; Killen et al., 2007):

- thermal desorption,
- photon-stimulated desorption (PSD),
- ion sputtering,

and

- micro-meteorite impact vaporisation.

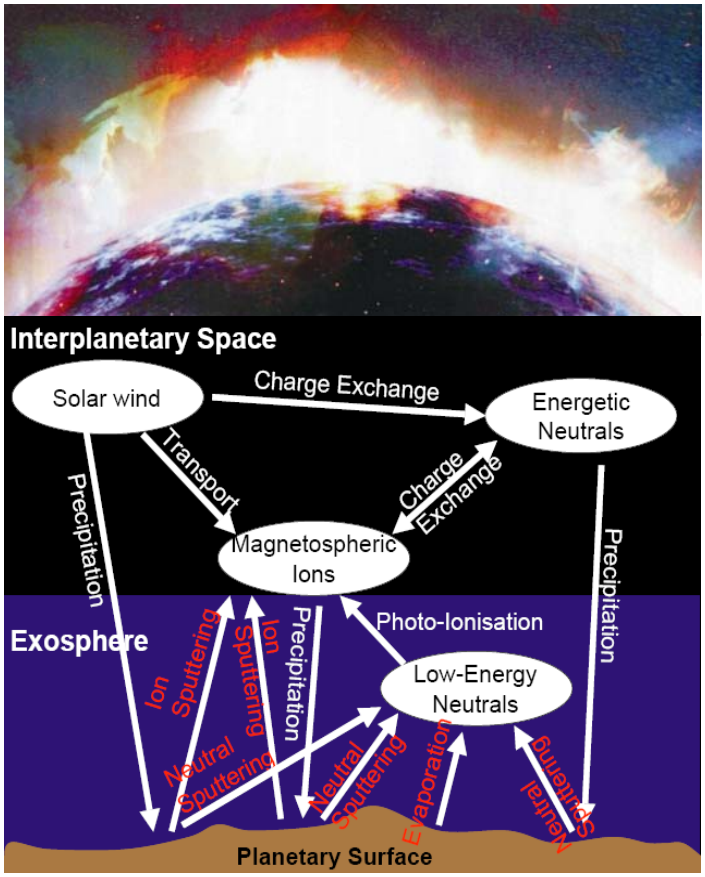

Figure 1: Illustration of various solar radiation and plasma interaction processes with Mercury's surface (e.g., Milillo et al., 2005).

The presently available information on the mineralogical composition including composition modelling of Mercury's surface can be used for applying a mineralogical model that serves as basis for the sputter related exosphere calculations. In the present study we concentrate on particle sputtering by the impact of solar wind protons on Mercury's surface, because this process releases surface elements more or less in a stoichiometric way into the exosphere.

2 Observational evidence of Mercury's surface composition

Mercury's surface, especially its age, origin, evolution and composition are not well known at present, due to the lack of sufficient remote and in situ measurements and observations. Efforts have been carried out to estimate the planets surface composition by using spectral reflectance measurements in comparison with lab-based spectra of analogue materials. During the past decades optical and near-infrared spectra have been obtained (Warell, 2003). The infrared spectra of Mercury, combined with laboratory studies of analogue materials, indicate that the rock composition is dominated by feldspars and low iron pyroxene (Warell and Blewett, 2004). Burbine et al. (2002) used synthetic Mercury analogues to compare low-FeO anorthositic compositions with that of partial melts, derived from melting experiments of an enstatite-rich chondrite. In their work the compositions of basaltic partial melts and their residual aubritic materials were related to that of Mercury's crust and mantle. In other experiments Blewett et al. (1997) used lunar anorthositic breccia MAC 88105, which is related to lunar meteoroid material, as analogues to rocks of

Mercury's crust. One should note that the synthetic Mercury composition used by Burbine et al. (2002) is depleted in FeO relative to the lunar anorthosite MAC 88105.

The observed spectral reddening of the surface by space weathering can only be reproduced if the surface soils contain at least a few wt % of FeO in the bulk material (Hapke, 2001; Burbine et al., 2002). Furthermore, mid-infrared spectral studies of Mercury's surface indicate also Na-rich feldspars and pyroxene (Sprague and Roush, 1998) and alkali basalts (Sprague et al., 1994), as well as clino-pyroxene (Sprague et al., 2002).

Table 1. Modelled mineralogical surface composition of Mercury (Wurz et al., 2008).

Mineral	Chemical composition	Mineral abundance
iron/nickel metal	Fe, Ni	0.07%
troilite	Fe S	0.15%
daubreelite	$Fe\ Cr_2\ S_4$	0.15%
Oldhamite	Ca S	0.15%
sphalerite	Zn S	0.58%
Feldspar group		
albite	$Na\ Al\ Si_3\ O_8$	17.44%
K feldspar	$K\ Al\ Si_3\ O_8$	0.39%
anorthite	$Ca\ Al_2\ Si_2\ O_8$	8.72%
ilmenite	$Fe\ Ti\ O_3$	0.07%
Apatite	$Ca_5\ (P\ O_4)_3\ (OH, F, Cl)$	1.45%
Pyroxene group		
Wollastonite	$Ca\ Si\ O_3$	2.91%
Ferrosilite	$Fe_2\ Si_2\ O_6$	0.36%
enstatite	$Mg_2\ Si_2\ O_6$	29.06%
olivine group		
Fayalite	$Fe_2\ Si\ O_4$	2.18%
Fosterite	$Mg_2\ Si\ O_4$	36.33%

Finally, Mercury's soil analogues, which fit the spectroscopic observations, range from Lunar meteoritic material up to mixtures of Mercury analogue materials like labradorite and enstatite. Based on the available mineralogical information Wurz et al. (2008) developed a mineralogical model of Mercury's surface. This model is in agreement with Goettel (1988) and can be considered as a global model since the present knowledge of the local mineralogy is not well known. Additionally to the mineralogical component we have constraints related to the mineralogical composition which arise from exosphere observations, in particular for Na, K, and Ca. For the three mineralogical groups (feldspar, pyroxene, olivine) Wurz et al. (2008) used a mixture of their end members for defining a mineralogical model of Mercury's surface shown in Table 1 from where an elemental composition of the surface is obtained by compositional modeling.

2.1 Compositional modelling

For investigating the differences between classical statistical methods and more realistic compositional modelling we produce intermediate compositions by using the perturbation mechanism procedure for the data of Mercury's surface. In early works compositional data analysis was based on correlation methods and Euclidean space geometry where one has to deal with absolute compositional values of individual entries. However, these methods do not exploit the full potential of the available data. The correlation coefficients between fixed pairs of elements and the Euclidean distance between two samples are both substantially influenced by normalization to a constant sum. According to Aitchison (1986) this is why classical statistical techniques may be misleading and are inappropriate for dealing with compositional data.

To account for the relative nature of compositional data, ratios among entries are considered rather than absolute values (Aitchison, 1986). The log-ratio methodology for compositional data analysis introduced by Aitchison (1986) has also been successfully applied for the interpretation of chemical data of the Martian surface (Kolb et al., 2006). The composition is defined as a collection of D non-negative

measurements, which sum to unity or 100 % per weight, volume, or abundance. Constraints are obeyed by the Simplex space geometry representing a *D*-dimensional analogue of a triangle, compared to the *D*-dimensional orthogonal Euclidean space geometry. A subset of the chemical constituents that are present in a sample normalized to a constant sum (e.g. 100 %) can be referred as a "subcomposition". In the sense of Aitchinson (1986) chemical compositions returned from space missions should be considered as sub-compositions.

To model the exchange of chemical compositions, Aitchison (1986) proposed the so-called *perturbation* mechanism, symbolized by the $\oplus$ sign shown in Equation (1). By means of the so called perturbation vector **p** the chemical composition $\boldsymbol{C}$ yields the chemical composition $\boldsymbol{C}^*$,

$$\mathbf{C}^* = \mathbf{p} \oplus \mathbf{C} = Cl\left(\left[p_1 c_1, p_2 c_2, \ldots, p_D c_D\right]\right) = \left[\frac{p_1 c_1}{\sum_{i=1}^{D} p_i c_i}, \frac{p_2 c_2}{\sum_{i=1}^{D} p_i c_i}, \ldots, \frac{p_D c_D}{\sum_{i=1}^{D} p_i c_i}\right], \qquad (1)$$

where $Cl(\cdot)$ corresponds to the closure or normalization operation. The components of the perturbation vector are a measure of change for the same parts of compositions linked by this vector. By using the log-ratio methodology (see also Wurz et al., 2008) this change is modeled in a multiplicative way, rather in the additive way which is applied by the traditional statistical techniques.

The chemical sub-compositions of Mercury's surface model (Table 1) in terms of element wt % consist of 15 elements (O, Na, Mg, Al, Si, P, S, K, Ca, Ti, Cr, Fe, Ni, Zn, OH). The detailed steps of our model approach are described in Wurz et al. (2008). But we note that when one produces intermediate compositions the elements which are not simultaneously present in all some compositions appear as a "0" in this composition. To avoid the effect related to "0" in the perturbation mechanism procedure, the intermediate sub-composition is calculated and then the rest of elements are imputed. By calculating the intermediate composition of the pyroxene group shown in Table 1, one deals with the minerals $Ca\,Si\,O_3$, $Fe_2\,Si_2\,O_6$, and $Mg_2\,Si_2\,O_6$. In such a case the compositions are formed by Si, O, Ca, Fe and Mg. We produce the intermediate composition for the group by applying the perturbation mechanism to the sub-composition Si and O and then, imputing the rest of elements in order to obtain the full composition (see also Martin-Fernández et al., 2003). The imputation method described in Martin-Fernández et al. (2003) guarantees that the ratios between the elements are preserved. Following this strategy the alternative estimates for the surface composition is obtained and given in Table 2.

Table 2. Correlation method compared to compositional modelling (see also Wurz et al., 2008).

Elements	Classical statistical method	Compositional modelling
Al	2.713 %	2.644 %
Ca	**1.670 %**	**0.780 %**
Cr	0.042 %	0.042 %
Fe	**0.872 %**	**1.720 %**
K	0.030 %	0.030 %
Mg	16.191 %	16.066%
Na	1.341 %	1.341 %
Ni	0.004 %	0.004 %
O	58.613 %	58.802 %
OH	0.069 %	0.069 %
P	0.208 %	0.208 %
S	0.519 %	0,529 %
Si	17.423 %	17.412 %
Ti	0.015 %	0.015 %
Zn	0.291 %	0.291 %

The ratio of Na/K on the surface is about 45, which is close to the lower vale of the range obtained observations in Mercury's exosphere (Killen et al., 2007). We use this value because in agreement with the recent work by Mura et al. (2008) we expect that the higher ratios resulting due to the enhancement of

Na in the exosphere by a combination of the PSD and sputtering processes. One can see from Table 2 that under the present model assumption the difference between the two methods is only relevant for two elements: Ca and Fe. Ca is about a factor 2 lower in the compositional model approach and Fe is more than twice times higher. Because Ca is presumably sputtered from Mercury's surface because of the large optical line-width, which can be interpreted as a temperature corresponding to about 12,000 K and the proximity of the observed Ca exospheric particles close to the polar areas of the planet where solar wind penetration may occur (Bida et al., 2000) we can investigate how strong the difference can effect the Ca exosphere density and which elemental composition may be in a better agreement with the observations.

3 Sputter model application

Particle sputtering will release all species from the surface into space reproducing more or less the local surface composition on an atomic level. The steady-state composition of the flux of sputtered atoms will correspond to the average bulk composition (e.g., Wurz and Lammer, 2003; Wurz et al., 2008). The energy distribution for particles sputtered from a solid, $f(E_e)$, with the energy E_e of the sputtered particle, has been given by Sigmund (1969):

$$f(E_e) = \frac{6E_b}{3-8\sqrt{E_b/E_c}} \frac{E_e}{(E_e+E_b)^3} \left\{1-\sqrt{\frac{E_e+E_b}{E_c}}\right\}, \quad (2)$$

where E_b is the surface binding energy of the sputtered particle and E_c is the cut-off energy. The cut-off energy, which is the maximum energy that can be imparted to a sputtered particle by a projectile particle with energy E_i, is given by the limit imposed by a binary collision between a projectile atom M_1 and the target atom M_2 (to be sputtered) as

$$E_c = E_i \frac{4M_1M_2}{(M_1+M_2)^2}. \quad (3)$$

The polar angle distribution of sputtered atoms, $f(\alpha)$ for fine-grained and porous regolith surfaces can be described by the following angular dependence, $f(\alpha) \sim \cos\alpha$ (Cassidy and Johnson, 2005). For the azimuth angle one can use a uniform distribution over 2π. Having the energy, the azimuth and elevation angle we calculate all three components of the initial particle velocity **v** and the trajectory of each sputtered particle. Using many such trajectories the vertical density profile $N_i(H)$ can be calculated (Wurz and Lammer, 2003; Wurz et al., 2008). Either the exospheric number density at Mercury's surface or the column density can be used for comparison with observational data.

The flux sputter flux Φ_i from the surface can be calculated as:

$$\Phi_i = \Phi_{ion} Y_i^{tot} = \Phi_{ion} Y_i^{rel} C_i, \quad (4)$$

where Φ_i is the ion flux onto the surface and Y_i^{tot} is the total sputter yield (e.g., Wurz et al., 2007; 2008) of species i ($C_i = C^*$, see Table 2) from Mercury's surface. One can calculate the exospheric density at the surface for species i as:

$$N_i(0) = \Phi_{ion} Y_i^{tot} \frac{1}{\langle v_i \rangle}, \quad (5)$$

where $N_i(0)$ is used in the Monte-Carlo calculation as a starting point to calculate the density profile from the sputtering process for a given surface composition.

If we model now the sputtered Ca density profile the large temperature of about 12,000 K (Bida et al., 2000) has to be interpreted as mean energy of 1.03 eV of the Ca atoms, which gives a binding energy of E_b = 2.1 eV in Equation (2). The results of our calculation for Ca together with two sets of Ca optical measurements (circles) from Bida et al. (2000) are shown in Figure 2. The solid line in Figure 2 corresponds to a Ca surface composition of about 1.67 %, while the dashed line corresponds to the two times lower composition value of about 0.78 %. One can see that the higher Ca content agrees much better with the observations.

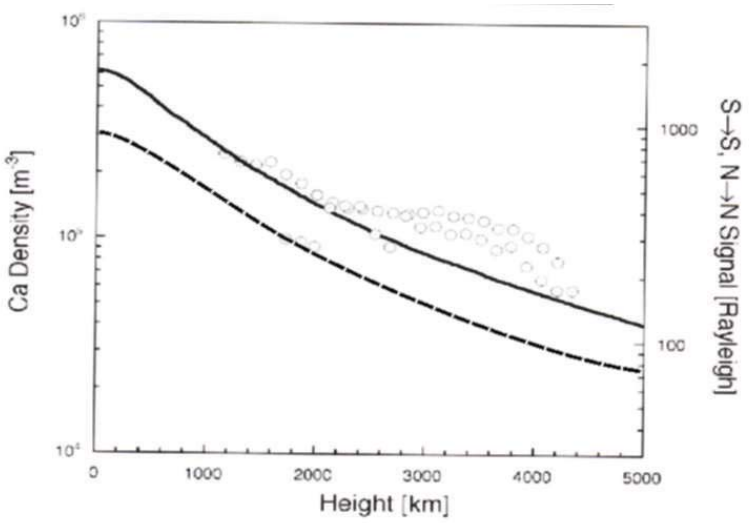

Figure 2: Comparison of calculated densities for sputtered Ca (solid and dashed lines) and observed densities (circles).

On the other hand it is clear that the composition modelling approach is more realistic. But one should also note that a detailed investigation on the solar wind parameters during the time when the exosphere observation was made has to be carried out. As pointed out by Bida et al. (2000, 2007) since Ca is sputtered from Mercury's surface by solar wind protons one can expect temporal as well as spatial variations of the Ca emission into the exosphere, which affects the measured data. It was reported by Bida et al. (2000) that the observed Ca corona was very dynamic. Killen et al. (2007) reported also the Ca column densities varied during the observations by a factor of about 1.6 from ~ 7.4×10^8 - 1.2×10^9 cm^{-2} which is close to the factor 2 difference obtained from the different composition model approaches.

This example shows nicely how composition modeling can help to advance our understanding of Mercury's surface composition but also how complex the situation is if one considers external influences triggered by the Sun. Therefore, it is important for future investigations that one starts well organized and exosphere observation campaigns where the solar wind and radiation environment during the exosphere observation is also coordinated so that the maximum of the scientific return can be obtained. In the future more elementals, which are in a very good agreement with exosphere observations, can be fixed to their corresponding values, when the composition modeling approach is applied. In such cases the model works only with the sub-composition of elements from where we have no information from ground- and space-based observations. This is possible due to the "multiplicative" method which is coherent with the sub-compositions. After the new model application the composition values of the remaining elements will change. After new observations of such elements in Mercury's exosphere are available, composition modeling method can again applied and the surface mineralogical surface model can be corrected or fine-tuned.

4 Conclusion

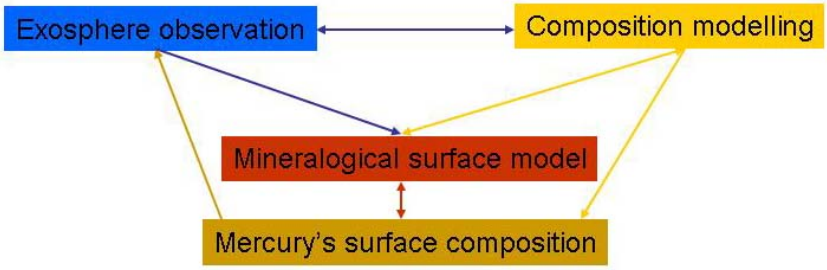

Figure 3: Illustration of the reconstruction of Mercuy's surface composition, due to exosphere and surface composition modelling.

In this study we outlined the relevance but also the difficulties of the multiplicative composition modelling method in connection to exosphere observations and mineralogical surface modelling of airless

bodies like Mercury. The developed common approaches in support of investigations of Mercury's exosphere and surface studies by instrumentation from the BepiColombo mission will be of great help in data interpretation. Although, there are uncertainties in the various contributions to Mercury's exosphere we can conclude that if in situ measurements of local particle densities by mass spectrometric means will be feasible, a global picture of Merury's surface composition should evolve via these remote observation techniques supported by theoretical exosphere and composition models.

Acknowledgements and appendices

H. Lammer, H. I. M. Lichtenegger and J. A. Martín-Fernández acknowledge support from the "Büro für Akademische Kooperation und Mobilität" of the Austrian Academic Exchange Service under the ÖAD-Acciones Integradas project 2006/2007. The chemical variability at planetary surfaces - implications for exogenic processes.

References

Aitchison, J. (1986). *The statistical analysis of compositional data*. Chapman and Hall Ltd, London: Blackburn Press.

Bida, T. A., Killen, R. M., Morgan, T. H. (2000). "Discovery of calcium in Mercury's atmosphere." *Nature 404*, 159 – 161.

Blewett, D. T., Lucey, P.G., Hawke, B. R., Ling, G. G., Robinson, M. S. (1997). A Comparison of Mercurian Reflectance and Spectral Quantities with Those of the Moon. *Icarus 129*, 217 – 231.

Broadfoot, A. L., Shemansky, D. E., Kumar, S. (1976). Mariner 10: Mercury atmosphere. *Geophys. Res. Lett. 3*, 577 – 580.

Burbine, T. H., McCoy, T. J., Nittler, L. R., Benedix, G. K., Cloutis, E. A., Dickinson, T. L. (2002). Specta of extremely reduced assemblages: Implications for Mercury, Met. Plan. *Science 37*, 1233 – 1244.

Cassidy, W., Johnson, R. E. (2005). Monte Carlo model of sputtering and other ejection processes within a regolith. *Icarus 176*, 499 – 507.

Goettel, K. A. (1988). Present bounds on the bulk composition of Mercury: Implications for planetary formation processes. In F. Vilas, C. Chapman, and M. Matthews (Eds.), *Mercury*, pp. 613 - 621. Tucson: University of Arizona Press.

Hapke, B. (2001). Space weathering from Mercury to the asteroid belt. *J. Geophys. Res. 106*(E5), 10,039 –10,074.

Harmon, J. K., Slade, M. A. (1992). Radar mapping of Mercury - Full-disk images and polar anomalies. *Science 258*, 640 – 643.

Harmon, J. K., Perillat, P. J., Slade, M. A. (2001) High-resolution radar imaging of Mercury's north pole. *Icarus 149*, 1 – 15.

Killen, R. M., Morgan, T. H. (1993). Maintaining the Na atmosphere of Mercury. *Icarus 101*, 293 – 312.

Killen, R. M., Ip, W.-H. (1999). The surface-bounded atmospheres of Mercury and the Moon. *Rev. Geophys. 37*(3), 361 – 406.

Killen, R., Cremonese, G., Lammer, H., Orsini, S., Potter, A. E., Sprague, A. L., Wurz, P., Khodachenko, M. L., Lichtenegger, H. I. M., Milillo, A., Mura, A. (2007). "Processes that promote and deplete the exosphere of Mercury." *Space Science Rev. 132*, 433 – 509.

Kolb, C., Martín-Fernández, J. A., Abart, R., Lammer, H. (2006). The chemical variability at the surface of Mars. *Icarus 183*(1), 10 – 29.

Lammer, H., Wurz, P., Patel, M. R., Killen, R., Kolb, C., Massetti, S., Orsini, S., Milillo, A. (2003). The variability of Mercury's exosphere by particle and radiation induced surface release processes. *Icarus 166*, 238 – 247.

Lewis, J. S. (1988). Origin and composition of Mercury. In F. Vilas, C. Chapman, and M. Matthews (Eds.), *Mercury*, pp. 651 - 666. Tucson: University of Arizona Press.

Martín-Fernández, J. A., Barceló-Vidal, C, Pawlowsky-Glahn, V. (2003). Dealing with zeros and missing values in compositional data sets. *Mathematical Geology 35*, 253 - 278.

Milillo, A., P. Wurz, S. Orsini, D. Delcourt, E. Kallio, R.M. Killen, H. Lammer, S. Massetti, A. Mura, S. Barabash, G. Cremonese, I.A. Daglis, E. DeAngelis, A.M. Di Lellis, S. Livi, V. Mangano, and K. Torkar (2005). Surface-exosphere-magnetosphere system of Mercury. *Space Sci. Rev. 117*, 397 – 443.

Mura, A., Wurz, P., Lichtenegger, H.I.M., Lammer, H., Milillo, A., Schleicher, H., Massetti, S., Orsini, S. (2008). The sodium exosphere of Mercury: Comparison between observations during Mercury's transit and model results. *Icarus* submitted.

Ness, N. F., Behannon, K. W., Lepping, R. P., Whang, Y. C., Schatten, K. H. (1974). Magnetic field observations near Mercury: preliminary results from Mariner 10. *Science 185*, 151 – 160.

Ness, N. F., Behannon, K. W., Lepping, R. P., Whang, Y. C., Schatten, K. H. (1976). Observations of Mercury's magnetic field. *Icarus 28*, 479 – 488.

Potter, A., Morgan, T. (1985). Discovery of sodium in the atmosphere of Mercury. *Science 229*, 651-653.

Potter, A. E., Morgan, T. H. (1997a). Evidence for suprathermal sodium on Mercury. *Adv. Space Res. 19*, 1571 – 1576.

Potter, A. E., Morgan, T. H. (1997b). Sodium and potassium atmospheres of Mercury. *Planet. Space Sci. 45*, 95 – 100.

Sprague, A. L., Kozlowski, R. W. H., Witteborn, F. C., Cruikshank, D. P., Wooden, D. H. (1994). Mercury: Evidence for anorthosite and basalt from mid-infrared (7.3-13.5 micrometers) spectroscopy *Icarus 109*, 156 – 167.

Sprague, A. L., Hunten, D. M., Lodders, K. (1995). Sulfur at Mercury, elemental at the poles and sulfides in the regolith. *Icarus 118*, 211 – 215.

Sprague, A. L., Kozlowski, R. W. H., Hunten, D. M., Schneider, N. M., Domingue, D. L., Wells, W. K., Schmitt, W., Fink, U. (1997). Distribution and Abundance of Sodium in Mercury's Atmosphere, 1985-1988. *Icarus 129*, 506 – 527.

Sprague, A. L., Roush, T. L. (1998). Comparison of laboratory emission spectra with Mercury telescopic data. *Icarus 133*, 174 - 183.

Sprague, A. L., Emery, J. P., Donaldson, K. L., Russell, R. W., Lynch, D. K., Mazuk, A. L. (2002). Mercury: Mid-infrared (3-13.5 μm) observations show heterogeneous composition, presence of intermediate and basic soil types, and pyroxene. *Meteo. & Planet. Sci. 37*, 1255 – 1268.

Starukhina, Larissa V., Shkuratov, Yurij G. (2000). The Lunar poles: Water ice or chemically trapped hydrogen? *Icarus 147*, 585 – 587.

Warell, J. (2003) "Properties of the hermean regolith: III. Disk-resolved vis-NIR reflectance spectra and implications for the abundance of iron." *Icarus 161*, 199 – 222.

Warell, J., Blewett, D. T. (2004). "Properties of the Hermean regolith: V. New optical reflectance spectra comparison with lunar anorthosites, and mineralogical modelling." *Icarus 168*, 257 – 276.

Wurz, P., Lammer, H. (2003) "Monte-Carlo Simulation of Mercury's Exosphere". *Icarus 164*(1), 1 – 13.

Wurz, P., Rohner, U., Whitby, J. A., Kolb, C., Lammer, H., Dobnikar, P., Martín-Fernández, J. A. (2007). The Lunar exosphere: The sputtering contribution. *Icarus 191*, 486 – 496.

Wurz, P., Whitby, J. A., Rohner, U., Martín-Fernández, J. A., Lammer, H., Kolb, C. (2008). The sputter contribution to Mercury's exosphere. *Icarus* submitted.